# Intrinsic Isotopic Selectivity Factors: $CO_2$ TEA Laser Photolysis of $CF_2Cl_2$

**David S. King* and John C. Stephenson**

*Contribution from the Laser Chemistry Program, National Bureau of Standards, Washington, D.C. 20234.* *Received April 10, 1978*

**Abstract:** The first real-time determination of isotopic selectivities in a pulsed IR photolysis is reported. In situ detection of nascent $CF_2$ photofragments by UV laser-excited fluorescence gave the probability of $CF_2$ production from $CF_2Cl_2$ samples of natural (98.9% $^{12}C$) and enriched (92.0% $^{13}C$) carbon-13 abundance. These measurements gave the probability, $^{12}P$ or $^{13}P$, of a $^{12}CF_2Cl_2$ or $^{13}CF_2Cl_2$ reactant dissociating into a $^{12}CF_2$ or $^{13}CF_2$ photofragment, as a function of IR laser wavelength and fluence, prior to any energy exchange or scrambling processes. The maximum value for the selective collision-free dissociation of $^{12}CF_2Cl_2$ was $\alpha_0 = {}^{12}P/{}^{13}P = 460$; for $^{13}CF_2Cl_2$ the maximum value $1/\alpha_0 = {}^{13}P/{}^{12}P = 150$ was obtained.

## Introduction

Since the initial reports of successful isotopically selective dissociation of polyatomic molecules in intense infrared (IR) fields,[1] there has been an extensive effort to understand and to utilize this process for large-scale isotopic segregations. This method relies on the absorption of many IR photons by a single molecule and its subsequent decomposition either via a unimolecular process or as the result of a favorable collision. The attraction of this type of mechanism for isotopic segregation is determined by four major factors: (1) the probability of molecular (reactant) dissociation in an IR field of given intensity and frequency; (2) the intrinsic selectivity of the controlling absorption process or processes resulting in dissociation; (3) selectivity-degrading (i.e., scrambling) and nonselective (i.e., thermal and secondary) processes; (4) overall throughput and economic feasibility.

To date, all considerations of isotopically selective IR photolysis mechanisms have been based on the measurements of macroscopic parameters such as isotopic ratios of products and reactants from end product array analysis. The derived bulk isotopic enrichments $\beta_r$ and $\beta_r$ for the reactant and products[2] contain a complicated convolution of basic photophysics degraded by scrambling (e.g., collisional energy transfer between isotopic species) and nonspecific (e.g., thermal) processes. Lyman and Rockwood[3] have used these end product isotopic ratios and the degree of photolysis, $f$, to calculate a macroscopic selectivity factor

$$\alpha = \ln f / \ln f\beta_r$$

This macroscopic $\alpha$ is an experimental variable, as shown by trends in the derived values for $\alpha$, as a function of either degree of photolysis or reagent gas pressures and mixture ratios.

We present here a powerful alternative approach to evaluate isotopic effects in IR multiphoton initiated processes. Our technique involves the real-time determination of dissociation yields in situ by UV laser-excited fluorescence (LEF) spectroscopy on a pulse by pulse basis. All of our experiments have been performed in the absence of collisions in an attempt to obtain an understanding of the basic photophysics involved in the unimolecular decomposition of molecules in an intense IR field. We present our data in terms of the probability of a single molecule of isotopic composition $i$ undergoing a collision-free dissociation in an IR field of intensity $I_{IR}$ at frequency $\lambda_{IR}$ to form a particular product as

$$^iP(I_{IR},\lambda_{IR})$$

For fixed values of $I_{IR}$ and $\lambda_{IR}$ the ratio

$$\alpha_0\{I_{IR},\lambda_{IR}\} \equiv {}^{12}P/{}^{13}P$$

gives the isotopic selectivities inherent in this process. The quantity $\alpha_0$ is an intrinsic property of the parent molecule, related to its electrical and structural parameters, and does not depend on macroscopic experimental variables like gas pressure or number of laser pulses. It is not within the scope of this paper to attempt to quantitatively assess the effects of collisions with either absorbent or transparent partners. However, the importance of collisions is shown by comparison of our intrinsic selectivity factors to the macroscopic enrichments observed by others under various experimental conditions.

We shall present data obtained with $CF_2Cl_2$ (difluorodichloromethane), a system whose multiphoton IR dissociation has been extensively studied. Lyman and Rockwood used this system[3] as their example of carbon-12/carbon-13 segregation. Recently, Ritter and Freund[4a] and Ritter[4b] have demonstrated the possibility of employing natural-abundance $CF_2Cl_2$ as a source of $^{13}CF_2$ to be used as "building blocks" in the manufacture of isotopically labeled materials.

## Experimental Section[5]

The experimental apparatus and techniques used herein have been extensively described elsewhere.[6] In brief, static samples of neat $^iCF_2Cl_2$ of high carbon isotopic purity at 1–80 mtorr in a 400-cm$^3$ Pyrex reaction vessel were exposed to single pulses from a thyratron-fired $CO_2$ TEA laser (120-ns fwhm; ca. 0.25 J pulse$^{-1}$ single-line operation). A small fraction of the $CF_2Cl_2$ dissociated during the laser pulse, forming $CF_2$ fragments in the ground electronic state. The concentration of nascent $^iCF_2$ photoproduct was determined in real time, on a pulse by pulse basis, by the technique of laser-excited fluorescence spectroscopy. A frequency-doubled $N_2$-pumped dye laser (3-ns fwhm, 10 $\mu$J pulse$^{-1}$ at 261.7 nm) was tuned into a wavelength region of identical absorption by both $^{12}CF_2$ and $^{13}CF_2$ and synchronized, using a programmable digital delay generator (BNC Model 7030), to probe the photofragment population at a time $\tau_D = 150$ ns after the leading edge of the IR laser pulse, as shown in Figure 1. The single vibronic level (SVL) fluorescence from the laser-excited $\tilde{A}$ $CF_2(0,2,0)$ state was spectrally resolved by a $f/1.6$ UV monochromator to discriminate against laser scatter and fluorescence from vibrational interferences, detected with a photomultiplier tube and gated electronics and recorded digitally using a signal averager.

The temporal shape of the IR laser pulse was recorded with a Ge–Au detector which had a 4-ns response time. The same Ge–Au detector was used to determine when the UV pulse occurred, so that $\tau_D$ was always accurately known. A trace of $CO_2$ laser intensity as a function of time is shown in Figure 1A. This is a single pulse as detected by the Ge–Au detector and digitized in real time by a Biomation 8100 transient recorder with a 10 ns/channel resolution. Although the $CO_2$ pulse lasts 600 ns, 84% of the energy is contained in the first 150 ns. The UV pulse was recorded here for a time delay $\tau_D = 150$ ns.

The nascent $CF_2$ fragments were initially generated by the $CO_2$ laser pulse in a well-defined cylindrical geometry. The concentration

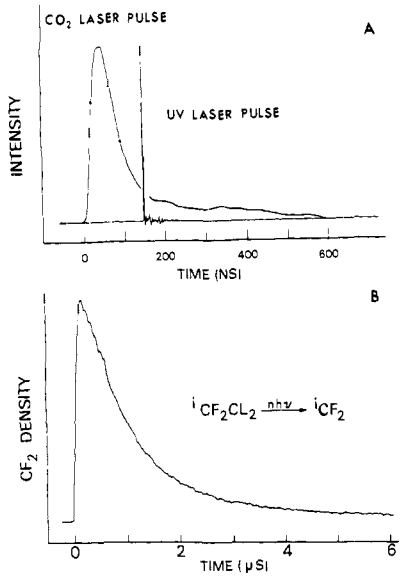


**Figure 1.** (A) IR and UV laser pulses. Each trace represents a single laser pulse, recorded in real time with a fast Au–Ge detector and a transient digitizer having 10-ns/channel resolution. The total IR pulse energy was 0.24 J on the 9.4 μm R(26) line. The UV pulse was obtained for a time delay $\tau_D$ = 150 ns after the leading edge of the $CO_2$ laser pulse. Approximately 84% of the total IR pulse energy is contained in the first 150 ns. (B) Laser-excited fluorescence signal from nascent $\tilde{X}$ $CF_2$ fragments formed in the ground vibrational level, as a function of time between the $CO_2$ photolysis pulse and the UV probe pulse. The $CO_2$ laser operated on the R(26) line of the 9.4 μm band, with an energy of 0.24 J/pulse.

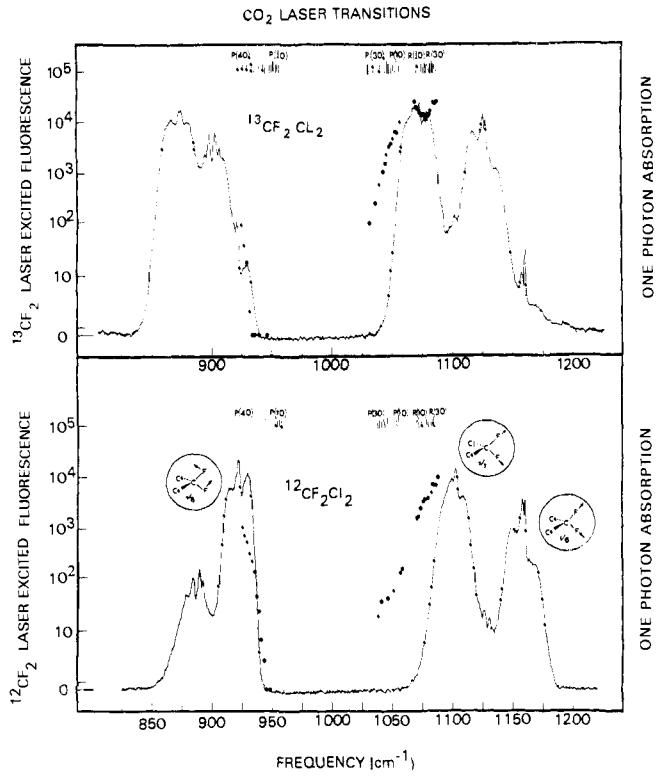


**Figure 2.** Isotopic effects of $CF_2Cl_2$ in the operational range of a $^{12}C^{16}O_2$ TEA laser. Continuous traces give linear one-photon absorption spectra of moderate pressure (ca. 5 torr) samples of $^iCF_2Cl_2$ at 2 cm$^{-1}$ resolution (Beckman IR-9). The $^{12}CF_2Cl_2$ sample exhibited natural carbon abundances (i.e., 98.9 ± 0.05% carbon-12) under mass spectroscopic analysis; the $^{13}CF_2Cl_2$ sample exhibited a carbon-13 content of 92.0 ± 0.15%. The points represent laser-excited $^iCF_2$ fluorescence data normalized according to eq 1 for UV laser intensity, sample pressure (which were in the range 1–80 mtorr) and isotopic composition, and an IR laser pulse fluence 30 J/cm$^2$ (215 MW/cm$^2$ peak intensity). The data represent quantitatively the amount of nascent $^iCF_2$ present in the dissociation region 150 ns after the leading edge of the $CO_2$ laser pulse (120 ns fwhm). The maximum signals correspond to conversions of about 25% of the $^{12}CF_2Cl_2$ and 60% of the $^{13}CF_2Cl_2$ in the region of high IR intensity into $^iCF_2$ during the first 150 ns (i.e., 84%) of the IR laser pulse.

of $CF_2$ at any later time, $\tau_D$, within this cylinder was probed by the UV laser pulse. The IR and UV beams propagated collinearly, but in opposing directions, through the cell. Both beams were loosely focused (30 cm focal length lenses) into the cell, and the beam waists of both lasers were constant in diameter over a distance of 2 cm at the focus. In this 2 cm long focal region, the radius of the IR beam was $4.7 \times 10^{-2}$ cm, while that of the UV beam was $5 \times 10^{-3}$ cm. The UV beam had a radius so much smaller than that of the IR photolysis pulse that only the central region, of constant IR intensity, was probed by the UV pulse. Also, the monochromator entrance slit was apertured so as to view only fluorescence from the middle 8 mm of the 2 cm long region of constant beam profile.

Only fragments in the path of the UV beam and in the vibrational ground state at time $\tau_D$ result in a LEF signal. By scanning the digital delay generator in time and recording LEF signal strengths, we observed directly the changes in $CF_2$ density due to reactant dissociation and collision-free diffusion of product from the narrow photolysis zone into the large cell. A maximum fragment density is observed at $\tau_D \approx$ 150 ns as shown in Figure 1B.

The UV probe laser excites near the band center of the $\tilde{A}$ $CF_2(0,2,0)$ ← $\tilde{X}$ $CF_2(0,0,0)$ transition for both isotopic species. The laser-excited $\tilde{A}$ $CF_2$ species immediately fluoresce ($\tau_0$ = 61 ns). Under all experimental conditions reported herein, there was no observable quenching of the $\tilde{C}F_2$ fluorescence and $\Phi_F$ = 1.0. The observed single vibronic level fluorescence signals, $\tilde{A}$ $CF_2(0,2,0) \rightarrow \tilde{X}$ $CF_2(0,2,0)$, can be directly related, by well-known spectroscopic formalism,[6] to absolute $^iCF_2$ concentrations.

Each determination of $^iP$ was based on the summation of 50 successive experiments. The samples were renewed every 100 pulses. However, no significant change in signal was observed between pulses 1 and 100 (the ratio of photolysis volume to cell volume was 1/4000 for our experiments).

Initially, samples of commercial grade $CF_2Cl_2$ (Matheson >99.0% chemical purity, natural isotopic abundance) were used as the source of $^{12}CF_2Cl_2$. However, even after gas chromatographic attempts to purify the commercial reactant, we observed interferences from residual non-$CF_2Cl_2$ halocarbon impurities at the $10^{-3}$ level. The measurements reported below were performed with samples of 92.0% carbon-13 content synthesized[4b] from $^{13}CCl_4$ and 98.9% carbon-12 synthesized from natural-abundance $CCl_4$.

## Results and Discussion

**Spectroscopy. Multiphoton Yield vs. One-Photon Absorption.** The linear one-photon infrared absorption spectra of $^{12,13}CF_2Cl_2$ obtained at a resolution and absolute frequency accuracy of 2 cm$^{-1}$ (Beckman IR-9) are presented in Figure 2. The $^{12}CF_2Cl_2$ sample exhibited natural isotopic abundances (i.e., 98.9 ± 0.05% carbon-12) under mass spectroscopic analysis, and the $^{13}CF_2Cl_2$ sample had a carbon-13 content of 92.0 ± 0.15%. Three strong, infrared-active normal modes are observed in the region of $CO_2$ laser transitions. The lowest frequency normal mode, $\nu_8$, corresponds to the $CF_2$ rocking motion. It appears as a doublet due to Fermi resonance with a lower frequency mode. The $\nu_1$ normal mode corresponds[7] to the CF symmetric stretching motion, and $\nu_6$ corresponds to the CF asymmetric stretch.

We have used real-time laser-excited fluorescence to probe the in situ production of nascent $CF_2$ formed in the collision-free IR dissociations of $^iCF_2Cl_2$ for all available $CO_2$ lasing transitions between 920 and 1088 cm$^{-1}$. The observed LEF signals are related[6] to the probability $^iP$ for production of $^iCF_2$ fragments from $^iCF_2Cl_2$ at a particular $CO_2$ wavelength by

$$S = \mathrm{Ap}E_{UV}({}^{12}PN_{12} + {}^{13}PN_{13}) \quad (1)$$

$E_{UV}$ is the energy of the UV laser pulse and $N_{12}$ or $N_{13}$ is the number density of $^{12}CF_2Cl_2$ or $^{13}CF_2Cl_2$ reactants. The LEF

signals were always linear with $E_{UV}$ and $N_i$. Ap is an apparatus constant related to the efficiency of our optical system. Equation 1 may be used to deduce $^iP$ from the signals $S$ determined for our two different isotopic samples. Since Ap is known (vide infra), the absolute probabilities may be determined; otherwise, only relative probabilities for dissociation may be deduced.

The dependence on $CO_2$ laser wavelength of $^iCF_2$ production from $CF_2Cl_2$ is shown in Figure 2. The data points represent the relative probabilities of forming $^iCF_2$ from $^iCF_2Cl_2$ with $CO_2$ pulses of 0.25 J (pulse shape shown in Figure 1A; 215 MW/cm$^2$ or 30 J/cm$^2$ peak intensity and fluence) at each $CO_2$ laser wavelength. It should be noted that in Figure 2 the multiphoton dissociation probabilities are plotted on a logrithmic scale while the classical absorption spectra are on a linear (i.e., percent transmission) scale.

The apparent structure in the IR multiphoton induced dissociation profiles follows the $^{12}CF_2Cl_2$ $\nu_8$ and $\nu_1$ and the $^{13}CF_2Cl_2$ $\nu_8$, $\nu_1$, and $\nu_6$ classical absorption spectra. Unfortunately, only a portion of the IR dissociation profile for any particular $^iCF_2Cl_2$ normal mode falls within the operating range of our $^{12}C^{16}O_2$ TEA laser. Maximum $^{12}CF_2$ production at the given IR fluence was observed for irradiation of $CF_2Cl_2$ at 1088 cm$^{-1}$ [R(36)], which was the highest frequency line our laser produced. Several $CO_2$ lasing transitions are highly effective for the collision-free dissociation of $^{13}CF_2Cl_2$. High yields of $^{13}CF_2$ are observed for irradiation of $^{13}CF_2Cl_2$ at either 1088 cm$^{-1}$ [R(36)] or 1075 cm$^{-1}$ [R(8)].

We estimate the $^{13}CF_2Cl_2$ $\nu_1$ dissociation probability profile to peak near 1070 cm$^{-1}$. This represents a red shift of ca. 7 cm$^{-1}$ relative to the linear absorption maximum. For $^{12}CF_2Cl_2$ $\nu_1$, the dissociation probability would peak at some frequency greater than 1088 cm$^{-1}$. The $CO_2$ laser does not go to low enough frequencies to permit determination of the dissociation maximum for the $\nu_8$ vibration of either isotope.

The observed laser-excited $^iCF_2$ fluorescence signals may be converted to absolute $CF_2$ densities present in the probe region during the UV laser pulse. To do this, the efficiency, Ap, of our optical system was determined by measuring the LEF signal from a standard fluorescence source[8] (SVL fluorescence from benzene). The absorption coefficient of the $\tilde{A}$ $CF_2(020)$ $\leftarrow \tilde{X}$ $CF_2(000)$ transition is known,[9] and from the absorption coefficient, optical efficiency, and fluorescence quantum yield, the absolute number density of $CF_2$ fragments is easily calculated. For $^{12}CF_2Cl_2$ the largest $CF_2$ LEF signals observed at $\tau_D$ = 150 ns, for pulses of about 30 J/cm$^2$ (215 MW/cm$^2$ peak intensity), corresponded to conversions of about 25 ± 10% of the reactant to $CF_2$; for $^{13}CF_2Cl_2$ this number is about 60 ± 20%.

**Isotopic Selectivity.** The wavelength dependence of $\alpha_0$, the ratio of molecular dissociation probabilities, $^{12}P/^{13}P$, in an IR field of ca. 30 J/cm$^2$ (215 MW/cm$^2$ peak intensity) under collision-free conditions is presented in Figure 3. Every $^{12}C^{16}O_2$ laser transition resulted in excitation processes that favored the collision-free multiphoton dissociation of one isotopic species of $CF_2Cl_2$ over the other. In no instance did we observe a value $\alpha_0$ = 1.0. The derived isotopic selectivities, $\alpha_0$, varied in a smooth fashion within each $CO_2$ laser branch. Within the spectral region associated with a specific molecular vibration, excitations to the blue favored the selective dissociation of the lighter isotopic species; excitations to the red favored the heavier one.

Molecular dissociation probabilities for $^{12}CF_2Cl_2$ in excess of 100 times $^{13}P(\lambda_{IR},I_{IR})$ were achieved for $\lambda_{IR} \approx 10.7$ μm (the P(32) to P(24) $CO_2$ lines at 933 to 940.5 cm$^{-1}$). A maximum value of $\alpha_0(12/13) \gtrsim 460$ was observed at 935 cm$^{-1}$ (the P(30) line). The value of 460 represents a lower limit due to the limit of accuracy in determining actual isotopic compositions $^iCF_2Cl_2$. The accuracy of our determination of the other values

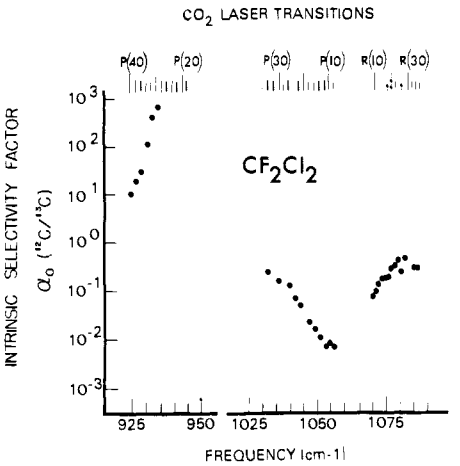


**Figure 3.** Ratios of molecular dissociation probabilities for $^{12}CF_2Cl_2/^{13}CF_2Cl_2$ at each $^{12}C^{16}O_2$ lasing transition. The points were derived from laser-excited $^iCF_2$ fluorescence data, normalized via eq 1 for UV laser intensity, sample pressure (in the range 1–80 mtorr) and IR laser fluence (30 J/cm$^2$, 215 MW/cm$^2$ peak intensity). Samples of 98.9% carbon-12 and 92.0% carbon-13 content were used. The data point at the 935-cm$^{-1}$ P(30) line represents a lower limit on $\alpha_0$(P(30)) due to uncertainties in reactant isotopic compositions (i.e., $\alpha_0(10.7\ \mu m) \gtrsim 460$). The accuracy of the $\alpha_0$ determinations is about 15%. Ratio values for the 10.6-μm P-branch $CO_2$ lines higher in frequency than the P(30) line are limited by signal to noise.

of $\alpha_0$ in Figure 3 is approximately 15%. Presumably for the P(30) to P(20) lines (these points are not shown in Figure 3) the intrinsic value of $\alpha_0$ increases beyond 460; however, the relative $^{12}CF_2$ yields are very low and calculated values for $\alpha_0$ are determined by signal-to-noise limiting factors. Carbon-13 enriched $CF_2$ may be generated with intrinsic selectivities of $50 < 1/\alpha_0 < 150$ by irradiation at 9.6 μm (the P(8) to P(28) $CO_2$ lines at 1057 to 1039 cm$^{-1}$). The optimum IR wavelength for the selective dissociation of $^{13}CF_2Cl_2$ is 1057 cm$^{-1}$ (the P(8) line) where $1/\alpha_0 = 153$.

**Intensity Dependence.** During the course of this and related work, we have investigated the functional dependences of molecular dissociation probabilities, for various reactant species, on IR laser pulse characteristics. Figure 4 presents relative $^iCF_2$ LEF signals observed ($\tau_D$ = 150 ns) following the dissociation of low-pressure samples of $^iCF_2Cl_2$ by the 9.2 μm R(26) $CO_2$ laser line. The $^{12}CF_2Cl_2$ was photolyzed while flowing at 10 mtorr; the $^{13}CF_2Cl_2$ was photolyzed while static at pressures between 5 and 10 mtorr. The IR pulse was attenuated using a 7.5 cm long cell containing a varied amount of $CF_2Br_2$ (1–10 torr) plus $N_2$ to 700 torr of total pressure. The dependence on $CO_2$ pulse energy of $^iCF_2$ production from $^iCF_2Cl_2$ (i.e., $^iP$) is the same for both isotopes over the range 0.24–0.015 J pulse.$^{-1}$ That is, as the pulse energy varied by a factor of 16, the ratio

$$\alpha_0(\lambda_{IR},I_{IR}) = {}^{12}P(\lambda_{IR},I_{IR})/{}^{13}P(\lambda_{IR},I_{IR})$$

was constant to within ±10%, independent of $CO_2$ pulse energy.

## Conclusions

$CF_2Cl_2$, following the absorption of several (i.e., 26–30) IR photons, may dissociate (eq 2 and 3) even in the absence of

$$CF_2Cl_2 + nh\nu \rightarrow CF_2 + Cl_2 \qquad \Delta H = 74 \text{ kcal} \quad (2)$$

$$CF_2Cl_2 + nh\nu \rightarrow CF_2Cl + Cl \qquad \Delta H = 78 \text{ kcal} \quad (3)$$

collisions. Previous estimates of the branching ratio[10-12] for these two decomposition mechanisms have placed the probability of molecular elimination in the decomposition of $CF_2Cl_2$

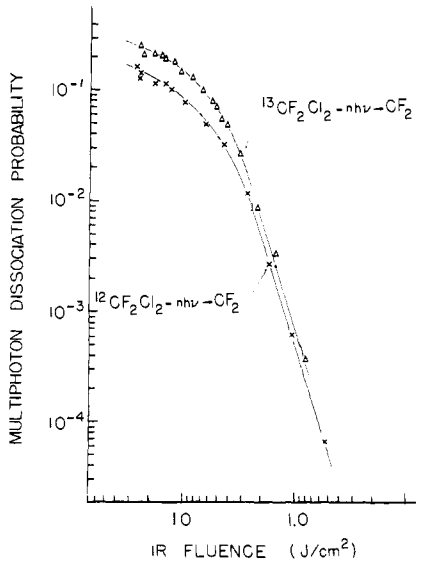


**Figure 4.** Laser-excited fluorescence from nascent $^iCF_2$ fragments formed in the collision-free IR dissociation of $^iCF_2Cl_2$ as a function of $CO_2$ laser pulse energy. The $CO_2$ TEA laser operated at 9.2 $\mu$m (the R(26) line). The geometry of the dissociating and probe beams is described in the text. The data points have been corrected to reflect 100% isotopic purities. The horizontal axis represents the fluence during the initial 150 ns (i.e., 84%) of the IR pulse. The vertical scale factors give absolute conversion probabilities $^iP(9.2\ \mu m, I_{IR})$ of $^iCF_2Cl_2$ to nascent $^iCF_2$ fragments as measured at $\tau_D$ = 150 ns in the region of highest IR intensity probed by the UV laser.

(2) in the range 2–15%. It has been demonstrated[10] that at pressures in excess of 0.5 torr the apparent branching ratio for channel 2, as determined by end product array analysis, may vary from near zero to unity depending on specific thermal and secondary photochemical effects. On the basis of real-time LEF signals observed in situ at $\tau_D$ = 150 ns, we would estimate a maximum probability of $CF_2$ formation in the collision-free IR laser-driven dissociation of $^{13}CF_2Cl_2$ in the $\nu_1$ region to be $^{13}P_{max}(\nu_1) = 0.7 \pm 0.25$ for the 215 MW/cm$^2$, 30 J/cm$^2$ pulses described above. This is the value observed following dissociation at either the P(8) line at 1071 cm$^{-1}$ or the P(36) line at 1088 cm$^{-1}$—the two frequencies most favorable for $^{13}CF_2$ formation. This may be compared with the probability $^{12}P_{max}(\nu_8) = 0.036 \pm 0.02$ observed for $CF_2$ formation from the photolysis of $^{12}CF_2Cl_2$ at 10.8 $\mu$m (the P(36) line at 925 cm$^{-1}$). In the $\nu_8$ region of absorption, $^{12}CF_2Cl_2$ ($\nu_8$) exhibits nominally the same one-photon absorption at 929 cm$^{-1}$ as $^{13}CF_2Cl_2$ ($\nu_1$) at 1071 or 1088 cm$^{-1}$.

Comparison of our results on $CF_2$ production to the estimates[10-12] of the branching ratio for reactions 2 and 3 is complicated by the possibility of the prompt IR photolysis of $CF_2Cl$ produced in (3) to yield $CF_2$ + Cl, with the final result written

$$CF_2Cl_2 + nh\nu \rightarrow CF_2 + 2Cl \qquad (4)$$

Our experiment does not permit us to distinguish between processes (2) and (4) if both lead to immediate $CF_2$ formation (i.e., within our experimental 10-ns time resolution). We have previously[6] discussed reaction 4 and considered it an unlikely interference on the basis of the matrix-isolated infrared spectrum[13] of $CF_2Cl$. The nearest absorption feature of $CF_2Cl$ was identified at 1148 cm$^{-1}$ (8.71 $\mu$m), which seems too remote in frequency to be excited by the lower frequency $CO_2$ laser lines. Certainly, if prompt photolysis of the nascent $CF_2Cl$ were to occur under any circumstance, it would be much more likely for irradiations in the $\nu_1$ (9.4 $\mu$m) spectral region than the $\nu_8$ (10.8 $\mu$m) region. Indeed, a possible explanation for the observed $P_{max}(\nu_1, 215\ MW/cm^2)$ being 20 times $P_{max}(\nu_8, 215$ MW/cm$^2$) is that collision-free $CF_2$ formation from reaction 4 is very efficient for IR pulses of 30 J/cm$^2$ at 9.3 $\mu$m.

Bearing more directly on the mechanism(s) of $CF_2$ formation is the observation[6] that the total energy content in the nascent $CF_2$ and its distribution over internal (i.e., electronic, vibrational, and rotational quantum states) and translational degrees of freedom is independent of photolysis wavelength. The same results are observed for photolysis of $CF_2Cl_2$ ($\nu_8$) at 10.8 $\mu$m (the P(36) line at 929 cm$^{-1}$) and of $CF_2Cl_2$ ($\nu_1$) at 9.2 $\mu$m (the R(26) line at 1083 cm$^{-1}$). It seems improbable that this would occur if the $CF_2$ produced in one case came predominantly from mechanism 2 while the other case via (4). Unfortunately, our experiments which only monitor $CF_2$ production cannot determine unambiguously the branching ratio into channels 2, 3, or 4. Nevertheless, the results herein reported are accurate indicators of both the absolute amounts of $^iCF_2$ formed and the intrinsic isotopic selectivities available in the collision-free IR dissociation of $CF_2Cl_2$.

In an earlier work Lyman and Rockwood[3] reported carbon-12 isotopic enrichment observed in end product arrays following the $CO_2$ TEA laser photolysis at 10.6 $\mu$m (the P(20) line at 944 cm$^{-1}$) of $CF_2Cl_2$ diluted in $N_2$. Depending on initial pressure and degree of photolysis, they obtained average selectivity factors in the range $1.2 < \alpha < 3.6$ for the selective dissociation of $^{12}CF_2Cl_2$. Their highest selectivity was achieved for a sample of 0.1 torr of $CF_2Cl_2$ + 0.4 torr of $N_2$, and the selectivity decreased monotonically with increasing pressure. By photolysis of a large portion of the initial sample they observed carbon-13 enrichment in the unphotolyzed parent species.

Ritter and Freund[4a] irradiated mixtures of $CF_2Cl_2$ (~2 torr) in the presence of a coreagent (6–8 torr) to scavenge the $^iCF_2$ fragments. Following the dissociation at 10.8 $\mu$m (the P(36) line at 929 cm$^{-1}$) of 90% of the initial $CF_2Cl_2$ sample ($f$ = 0.1), they reported a 24-fold enrichment in the net carbon-13 content of the remaining reactant. Using the formalism of Lyman and Rockwood this reduces to an average macroscopic selectivity of $\alpha(10.8\ \mu m) \approx 5$ for the dissociation of $^{12}CF_2Cl_2$ compared to $^{13}CF_2Cl_2$, neglecting possible photolysis of the various product species.

The selective decomposition of $^{13}CF_2Cl_2$ was achieved[4a] for irradiation at 9.3 $\mu$m (the R(18) line at 1077 cm$^{-1}$). This represents one of the few experimental observations of selective enrichment of a rare isotopic species in a product array. The calculated selectivity for the decomposition of $^{13}CF_2Cl_2$ was

$$1/\alpha(9.3\ \mu m) \approx 1.04$$

In their work on carbon isotope separation[14] by multiphoton dissociation of $CF_3I$, Bittenson and Houston report pressure and temperature effects on macroscopic enrichments. Their technique employs the selective photolysis of $^{12}CF_3I$. By using low sample pressures and a cell temperature of −80 °C, they achieved carbon-12 selectivities of $\alpha \approx 40$, some 4–5 times greater than observed for room-temperature samples. The high isotopic enrichment factors they reported were due, in part, to the condensation of $I_2$, eliminating competitive nonselective processes.

Our results would predict an intrinsic selectivity of $\alpha_0(10.7\ \mu m) \approx 500$ for the Lyman and Rockwood experiment and values of $\alpha_0(10.8\ \mu m) = 30$ and $1/\alpha_0(9.3\ \mu m) \approx 5$ for the experiments of Ritter and Freund. For the first time it is now possible to compare quantitatively the results of various separation schemes. By utilizing a coreagent to scavenge the photolysis (and thermal) products, Ritter and Freund were able to realize a much higher degree of isotopic segregation than demonstrated previously, even though working at a less favorable IR wavelength. In point of fact, however, they only succeeded in isotopic segregations of one-fifth to one-sixth of

that intrinsically available in the multiphoton absorption process.

Significant increases in the overall efficiency of an isotopic segregation scheme may be achieved by irradiation of a low-pressure mixture of reactant in an excess of effective coreagent and by cooling the sample and reaction vessel. However, a greater increase in selectivity and end product enrichment could be realized by a more judicious choice of IR laser frequency or frequencies. Our technique allows us to rapidly assay relative isotopic dissociation probabilities and choose appropriate wavelengths to provide both high selectivity and high yields. Our studies only require microscopic quantities of isotopically enriched reagent (i.e., a few micrograms). In a system analogous to those of Ritter and Freund one should observe macroscopic isotopic segregations consistent with an average selectivity of $\alpha > 100$ for the dissociation of $^{12}CF_2Cl_2$ at 10.7 $\mu$m (the P(30) line at 934 $cm^{-1}$) and of $1/\alpha \approx 30$ for carbon-13 enriched product species at 9.5 $\mu$m (the P(8) line at 1057 $cm^{-1}$). These represent substantial increases over the values of 5 and 1.04 reported previously.

Very few attempts have been successful in the selective segregation of rare isotopes into product species using IR multiphoton dissociation techniques. As demonstrated by the work of Ritter and Freund, the low carbon-13 dissociation selectivities result in negligible product array enrichments; it is then preferable to dissociate >90% of the sample with selectivity for carbon-12 decomposition.

By using real-time LEF diagnostics to determine collision-free dissociation probabilities for each isotopic species, one can very rapidly assess optimum IR wavelengths for the selective multiphoton dissociation of rare isotopic species. This allows one to design experiments to selectively perturb those isotopic species of lesser abundance. Provided it is possible to scavenge the initially formed intermediates without encouraging secondary photolysis, scrambling, or nonselective thermal processes, one may realize a maximum isotopic enrichment of $^{13}\beta_{P,max} = R_p/R_0 = 1/\alpha_0$ for the products.

**Acknowledgment.** We gratefully thank Dr. Joseph J. Ritter for providing us with the isotopically enriched and synthetically purified samples of $^{i}CF_2Cl_2$ and the valuable assistance of Drs. J. J. Ritter, Richard E. Rebbert, and Marilyn Jacox in materials purification and analysis. This work received partial support from the Department of Energy under Contract No. EA-77-A-01-6010, task No. A-058.

## References and Notes

(1) R. V. Ambartsumyan and V. S. Letokhov, *Acc. Chem. Res.*, **10**, 61 (1977); V. S. Letokhov and C. B. Moore, *Sov. J. Quantum Electron. (Engl. Transl.)*, **6**, 129 (1976); C. D. Cantrell, S. M. Freund, and J. L. Lyman, "Laser Handbook", Vol. 3, M. Stitch, Ed., North-Holland Publishing Co. (to be published), and references therein.
(2) In keeping with the notation of Lyman and Rockwood,[3] we shall define the enrichment factor, $\beta_r$, for the reactant species as $\beta_r = R_r/R_0$, where $R_0$ is the normal isotope ratio and $R_r$ is the isotope ratio of the reactant remaining after irradiation. Likewise, the enrichment factor for the product species is given as $\beta_p = R_p/R_0$, where $R_p$ is now the isotope ratio of the products. We also define the selectivity factor, $\alpha$, by $dn_1/dn_2 = \alpha n_1/n_2$, where $n_1$ and $n_2$ are the concentrations of two isotopic species.
(3) J. L. Lyman and S. D. Rockwood, *J. Appl. Phys.*, **47**, 595 (1976).
(4) (a) J. J. Ritter and S. M. Freund, *J. Chem. Soc., Chem. Commun.*, 811 (1976); (b) J. J. Ritter, *J. Am. Chem. Soc.*, **100**, 2441 (1978).
(5) Certain commercial materials and equipment are identified in this paper in order to specify adequately the experimental procedure. In no case does such identification imply recommendation or endorsement by the National Bureau of Standards, nor does it necessarily imply that the material or equipment identified is necessarily the best available for the purpose.
(6) D. S. King and J. C. Stephenson, *Chem. Phys. Lett.*, **51**, 48 (1977); J. C. Stephenson and D. S. King, *J. Chem. Phys.*, **69**, 1485 (1978).
(7) J. Morcillo, L. J. Zamorano, and J. M. V. Heredia, *Spectrochim. Acta*, **22**, 1969 (1966); E. K. Plyer and W. S. Benedict, *J. Res. Natl. Bur. Stand.*, **47**, 202 (1951).
(8) C. S. Parmenter and M. W. Schuyler, *Chem. Phys. Lett.*, **6**, 339 (1970).
(9) D. S. King, P. K. Schenck, and J. C. Stephenson, "Spectroscopy and Photophysics of the $CF_2$ $A^1B_1 - X^1A_1$ System" (in process of publication).
(10) G. Folcher and W. Braun, *J. Photochem.*, **8**, 341 (1978).
(11) J. W. Hudgens, *J. Chem. Phys.*, **68**, 777 (1978).
(12) Aa. S. Sudbo, P. A. Schulz, E. R. Grant, Y. R. Shen, and Y. T. Lee, *J. Chem. Phys.*, **68**, 1306 (1978).
(13) D. E. Milligan, M. E. Jacox, J. H. McAuley, and C. E. Smith, *J. Mol. Spectrosc.*, **45**, 377 (1973).
(14) S. Bittenson and P. L. Houston, *J. Chem. Phys.*, **67**, 4819 (1977).

# Carbon-13 Magnetic Shielding from Beam-Maser Measurements of Spin–Rotation Interaction in Acetonitrile

**S. G. Kukolich,*[1a] G. Lind,[1a] M. Barfield,[1a] L. Faehl,[1b] and J. L. Marshall[1b]**

*Contribution from the Departments of Chemistry, University of Arizona, Tucson, Arizona 85719, and North Texas State University, Denton, Texas 76203.* *Received May 1, 1978*

**Abstract:** The $J = 1 \rightarrow 0$ transitions in $CH_3{}^{13}CN$ were observed using a beam maser spectrometer at 6-kHz line width (fwhm) and a $^{13}C$-enriched sample. The strongest component was observed with natural-abundance $CH_3{}^{13}CN$. Spectra of $CH_3{}^{12}CN$ were obtained at higher resolution using Ramsey's method of separated oscillating fields. For $CH_3{}^{12}CN$ we obtain $eqQ_N = -4224.4 \pm 0.7$ kHz, $C_N = 2.0 \pm 0.4$ kHz, $C_H = -0.6 \pm 0.4$ kHz, and a $J = 1 \rightarrow 0$ transition center frequency of 18 397 783.5 $\pm$ 0.7 kHz. For $CH_3{}^{13}CN$ the $J = 1 \rightarrow 0$ transition center frequency is 18 388 681.0 $\pm$ 2.0 kHz and we obtain $eqQ_N = -4224.6 \pm 1$ kHz and $C_N = 1.9 \pm 0.5$ kHz. The $^{13}C$ spin–rotation strength in $CH_3{}^{13}CN$ was determined in this study to be 3.6 $\pm$ 0.2 kHz and this leads to a value of $\sigma_\perp = -11 \pm 14$ ppm.

## I. Introduction

Rotational transitions and nitrogen quadrupole coupling in $CH_3CN$ were first reported[2] in 1950. It is a favorable molecule for microwave study because of its large dipole moment (~4 D). More recently, Lamb-dip spectra in the microwave region were obtained by Costain.[3] Beam-maser transitions in $CH_3CN$ and $CD_3CN$ were observed in our earlier work,[4] and D quadrupole and $^{14}N$ quadrupole coupling strengths were reported.

The relationship between spin–rotation tensor elements and magnetic shielding tensor elements has been discussed by

0002-7863/78/1500-7155$01.00/0 